

Calibration-Free Analysis of Surface Proteins on Single Extracellular Vesicles Enabled by DNA Nanostructure

Kaizhu Guo,¹ Zongbo Li,¹ Allison Win,¹ Roxana Coreas,² Gary Brent Adkins,¹ Xinpeng Cui,³ Dong Yan,⁴ Minghui Cao,⁵ Shizhen Emily Wang,⁵ Wenwan Zhong^{1,2*}

¹Department of Chemistry, University of California-Riverside, Riverside, CA 92521, USA

²Environmental Toxicology Graduate Program, University of California-Riverside, Riverside, CA 92521, USA

³Department of Statistics, University of California-Riverside, Riverside, CA 92521, USA

⁴Nanofabrication Facility, University of California-Riverside, Riverside, CA 92521, USA

⁵Department of Pathology; University of California San Diego; La Jolla, CA 92093, USA

*Corresponding author: E-mail: wenwan.zhong@ucr.edu (W. Zhong).

Supporting Information

Table of Contents

1. Supporting Methods

2. Table and Figures

Table S1. DNA sequences used in this study.

Fig. S1. Schemes of RCA and analysis of the long DNA products by agarose gel electrophoresis.

Fig. S2. AFM and SEM results for the DNF and the DNF grown on the EV.

Fig. S3. NTA analysis of DNF and non-DNF in various reaction time (0-5.5 hours).

Fig. S4. Real-time fluorescence of RCA.

Fig. S5. RCA efficiency in different ratio of dATP to biotin-dATP.

Fig. S6. NTA analysis, AFM image and TEM image of EV.

Fig. S7. Representative fluorescence microscopy images of the EVs labeled with different dye.

Fig. S8. Correlation of detectable EVs particles count with EVs concentration.

Fig. S9. Representative CFM images of different samples.

Fig. S10. Average particle count per image of EV labeled with DNFs using Ab-DNA conjugates and aptamer assisted Ab-DNA conjugates.

Fig. S11. Detection of EVs using dual color labeled.

Fig. S12. Comparison of the expression profiles, represented by the particle ratios, of 5 protein markers in the EV derived from COLO-1 cells.

Fig. S13. Representative fluorescence microscopy images of COLO-1-derived EVs.

Fig. S14. Comparison of the expression profiles of protein markers in the EV derived from MCF-7, MDA-MB-231, PDX, COLO-1, PC-3 and A549 cells.

Fig. S15. Representative fluorescence microscopy images of PC-3-derived EVs.

Fig. S16. Representative fluorescence microscopy images of A549-derived EVs.

Fig. S17. Representative fluorescence microscopy images of MCF7-derived EVs.

Fig. S18. Representative fluorescence microscopy images of MDA-MB-231-derived EVs.

Fig. S19. Representative fluorescence microscopy images of PDX-derived EVs.

Fig. S20. Particle count of EGFR⁻/HER2⁻ EVs, EGFR⁺/HER2⁻ EVs, EGFR⁻/HER2⁺ EVs and EGFR⁺/HER2⁺ EVs using dual marker colocalization simultaneously.

Fig. S21. Comparison of particle ratio for HER2 and EGFR on EVs using single DNF labeling to dual DNF labeling.

Fig. S22. Particle count ratio between DNFs and DiO of membrane proteins on EVs derived from breast cancer patient serum samples and healthy patient serum samples.

Fig. S23. Particle count of detectable EVs derived from breast cancer patient serum samples and healthy patient serum samples.

Fig. S24. Protein profiling of HER2 and CD44 in breast cancer patient and healthy patient serum samples.

1. Supporting Materials and Methods

1.1 Chemicals

MFGE8 protein, anti-EGFR antibody and epidermal growth factor (EGF) were purchased from Sino Biological. Anti-CD9 antibody, anti-mouse IgG, cholera toxin, hydrocortisone and poly-L-lysine coated glass slide were purchased from Sigma Aldrich. Anti-CD63 antibody and anti-CD44 antibody were purchased from Novus Biologicals. All oligonucleotides were purchased from Integrated DNA Technologies. Phi29 DNA polymerase was purchased from New England Biolabs. Dibenzocyclooctyne-PEG5-N-hydroxysuccinimidyl (DBCO-PEG5-NHS) ester was purchased from Click Chemistry Tools. All other chemicals, including anti-HER₂ antibody, penicillin streptomycin, DMEM/F-12, insulin, DMEM, biotin-14-dATP and fetal bovin serum (FBS), were purchased from ThermoFisher Scientific.

1.1 Fabrication of 6 × 3 multi-well chip

The multi-well chip was fabricated via pouring polydimethylsiloxane (PDMS) to the mold and curing the polymer in an oven (55 °C, overnight). The cured PDMS structure and a glass substrate were oxygen plasma treated and irreversibly bonded. The wells were washed with 1M NaOH, water, ethanol and dried by air. After that, the bottom of the well was modified with 10% (v/v) (3-Aminopropyl)triethoxysilane (APTES) in ethanol for 10 min at room temperature and washed for several times. The bottom of the well was then modified with 20 ng/μL MFGE8 protein or 15 μg/mL anti-CD63 antibody in EDC coupling buffer (40 μg/mL EDC (1-Ethyl-3-(3-dimethylaminopropyl)carbodiimide), 0.1 mM MES (4-morpholinoethanesulfonic acid), pH 4.7). The wells were blocked with 1% BSA (Bovine Serum Albumin) before sample loading.

1.2 DNA-protein conjugation

DBCO-PEG5-NHS ester was used as a linker for the conjugation. The protein first reacted with DBCO-PEG5-NHS at room temperature for 30 mins. Excess cross-linkers were then removed from DBCO-activated proteins with Zeba spin columns (40-kDa MWCO). The DBCO-activated proteins were mixed with azide-labeled RCA initiators at 4 °C overnight. The resulted conjugation was characterized using gel electrophoresis.

1.3 Circular probe preparation and rolling circle amplification (RCA) for construction of DNA nanoflower (DNF)

For circular probe preparation, the phosphorylated template for DNFs (0.6 μ M) and the initiator (1.2 μ M) were mixed and annealed in the hybridization buffer (20 mM Tris-HCl, 5 mM MgCl₂, 137 mM NaCl, pH 7.5) by heating at 95 °C for 5 min, followed by cooling to room temperature over 3 hrs. The annealed product was incubated with the T4 DNA ligase in the ligation buffer (50 mM Tris-HCl, 10 mM MgCl₂, 1mM ATP, 10mM DTT) at 37 °C for 3hrs. The reaction was terminated by heating the solution at 65 °C for 20 min. Exonuclease I and Exonuclease III were then added to digest the un-ligated, linear template and initiator overnight at 37 °C. The reaction was terminated by incubation at 80 °C for 20 min. The concentration of the resultant circular probe was quantified by Nanodrop.

For a typical RCA used in our work, 5 nM of the circular probe was incubated with 25 nM of the RCA initiator in the reaction buffer (50 mM Tris-HCl, 10 mM MgCl₂, 10 mM (NH₄)₂SO₄ and 4 mM DTT) at 37 °C for 30 min. Then, 80 μ M of dNTPs and 2.5 U/ μ L of phi29 DNA polymerase were added to grow the DNF at 37 °C for 1 hr.

1.4 Nanoparticle tracking analysis (NTA)

Particle concentration and size distribution of EVs, linear RCA product and DNA nanoflowers were measured by NanoSight NS300 using a low volume flow cell manifold and a 405 nm laser module. A video of 30–60 s duration was taken with a rate of 25 frame/s.

1.4 Gel electrophoresis

Gel electrophoresis for the confirmation of the growth of DNA long chain and DNA-antibody conjugation, and optimization of biotin-dATP ratio were carried out in 0.5% or 1.5% Agarose gel in 1 x TBE. The DNAs were stained by SYBR gold. The images were taken under a Spectroline® UV transilluminator.

1.5 Real-time fluorescence

The RCA reaction was monitored in 96-well PCR plated and controlled using a Bio-Rad CFX Connect Real-Time PCR Detection System. The reaction mixture was incubated at 37 °C and fluorescence curves were recorded at 30 s intervals.

1.6 Atomic force microscopy (AFM), transmission electron microscopy (TEM), and scanning electron microscopy (SEM)

Ten μL sample was deposited on a freshly cleaved mica for 10 min. Before imaging, the samples were rinsed with deionized water for 3 times and then dried by N_2 . AFM images were recorded in air under the tapping mode using a Dimension 5000 Scanning Probe Microscope. The images were flattened by NanoScope Analysis software.

TEM was carried out using a Tecnail2 TEM. The EVs were stained with 2% uranyl acetate, embedded in 1% methyl cellulose, dried at room temperature and deposited on formvar-carbon-coated EM grids for imaging.

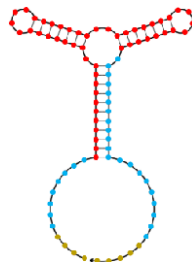
SEM was done with a Zeiss XB 1540 instrument. The sample solutions were prepared using the typical procedures for EV suspension and DNF labeling. Then 10 μL of each solution was

dropped on the silicon wafers which were soaked in piranha solution for 8 hrs, cleaned by ethanol and acetone sequentially, and dried before usage. The samples were dried again at 70 °C for 2 hrs, and coated by Ag sputtering before SEM imaging.

2. Table and Figures

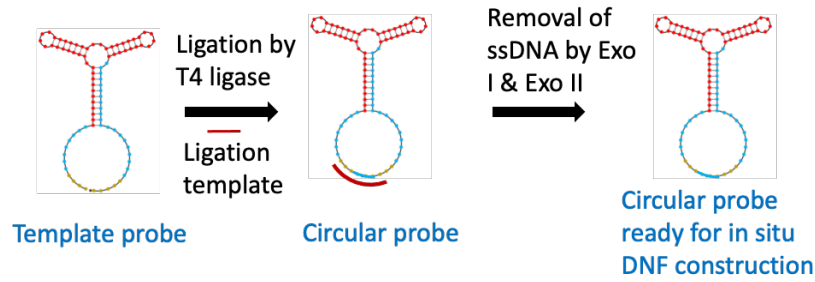
Table S1. DNA sequences used in this study. The initiators contain a target protein recognition domain (black), a trigger domain (blue) for growth of a DNF via RCA, and a spacer (grey) to connect the recognition domain and trigger domain. The sequences in red in the template probes are the regions initiating self-assembly into the DNF through the underline nucleotides.

Name	Sequences (5'-3')
Initiator 1 for RCA 1	CGT TGT CGT TAG TCT AGG ATT CGG CGT GTT AGC A
Initiator 2 targeting CD63 in RCA 1	CAC CCC ACC TCG CTC CCG TGA CAC TAA TGC TAA CAC GCC AGT CTA GGA TTC GGC GTG TTA GCA
Initiator 3 targeting HER2 in RCA 1	GCA GCG GTG TGG GGG CAG CGG TGT GGG GGC AGC GGT GTG GGG AGA GGT TAA GTT GTC GTT AGT CTA GGA TTC G
Template probe 1 for RCA 1	Phosphate-GAC TAA CGA CAA <u>CGC GTG TTA GCA AGC GAT ACG CGT</u> <u>ATC GCT ATG GCA TAT CGT ACG ATA TGC CTG CTA ACA CGC CGA</u> ATC CTA
Detection probe 1	CGA ATC CTA GAC TAA CG /3AlexF546N/
Initiator 4 for RCA 2	CCA TTA GAC CAC CAC CAG TCG AGA GAA GAT CAT AGC TT
Initiator 5 targeting HER2 in RCA 2	GCA GCG GTG TGG GGG CAG CGG TGT GGG GGC AGC GGT GTG GGG AGA GGT TAA CCA TTA GAC CAC CAC CAG TCG AGA GAA GAT CAT AGC TT
Template probe 2 for RCA 2	Phosphate-GTG GTC TAA TGG <u>AGA TCA TAG CTT AGA CGT TCC GGA</u> <u>ACG TCT CGC TCG TAA CTA GTT ACG AGA AGC TAT GAT CTT CTC</u> TCG ACT GGT G
Detection probe 2	TGG TGG TGG/3AlexF660N/

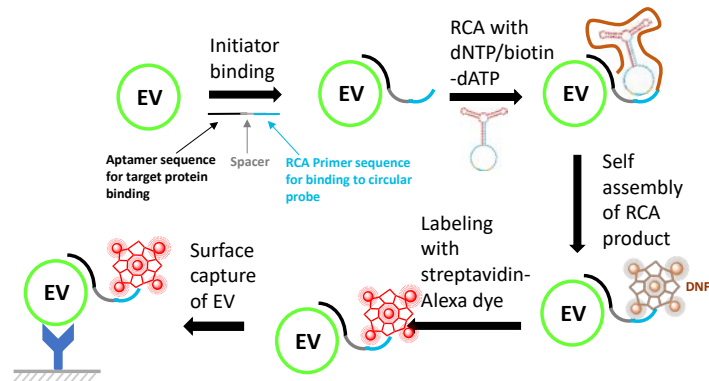


Predicted secondary structures of the template probe 2 for DNFs.

A



B



C

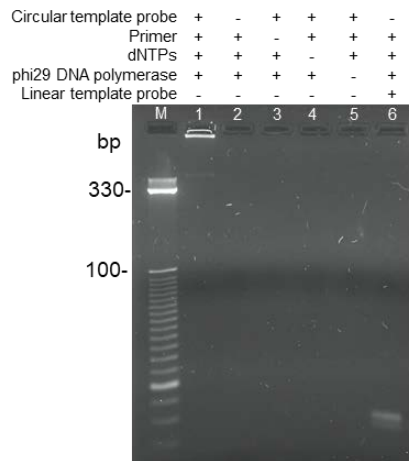
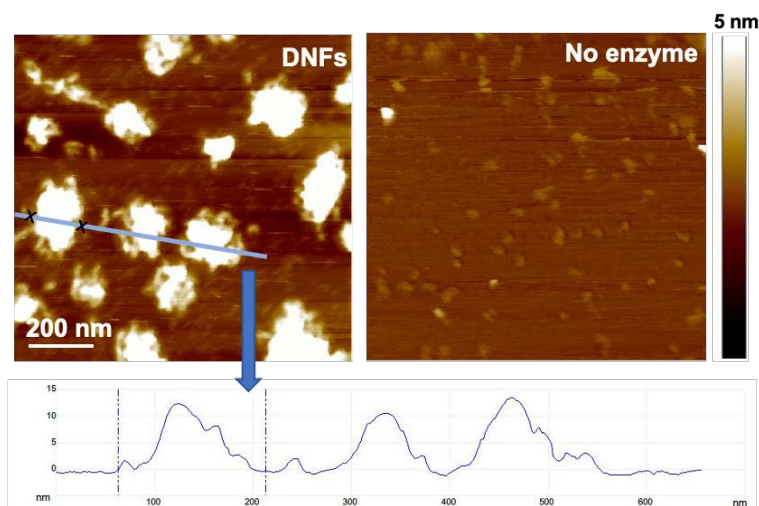


Fig. S1. Schematic illustration of (A) circular probe generation and (B) RCA on EV surface. (C) Scheme of Analysis of the long DNA products by agarose gel electrophoresis: Lane M: DNA marker; Lane 1: RCA product; Lane 2, 3, 4, and 5: reaction without circle template probe, initiator probe, dNTPs, phi29 DNA polymerase, respectively; Lane 6: reaction with linear template probe.

A



B

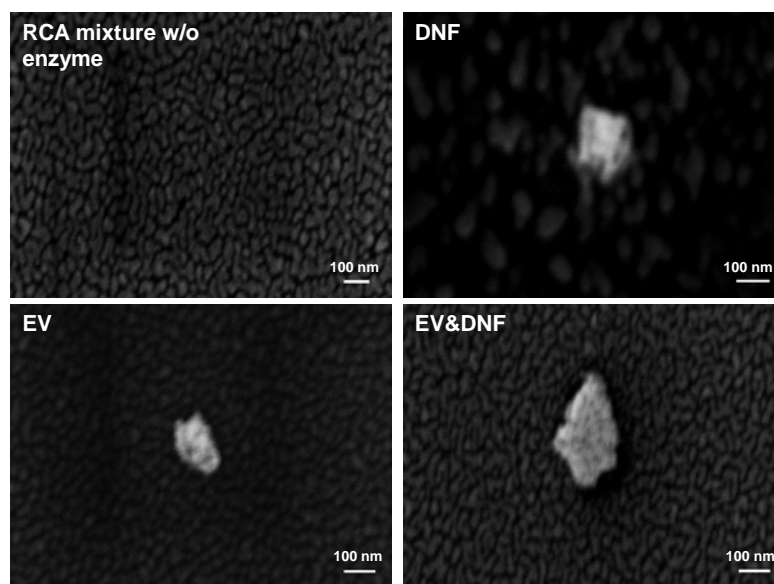


Fig. S2. (A) AFM images for the DNFs (left) and the reaction mixture with no enzyme added (right). The diameter of each globular DNF was measured to be $\sim 100 - 150$ nm (bottom). (B) SEM results for the DNF and its control - RCA mixture with no enzyme; as well as the EV and the DNF grown on the EV. Both the DNF and the EV only showed structures with diameters around 100 nm; but the sample that grew the DNF on the EV showed structures > 250 nm after drying.

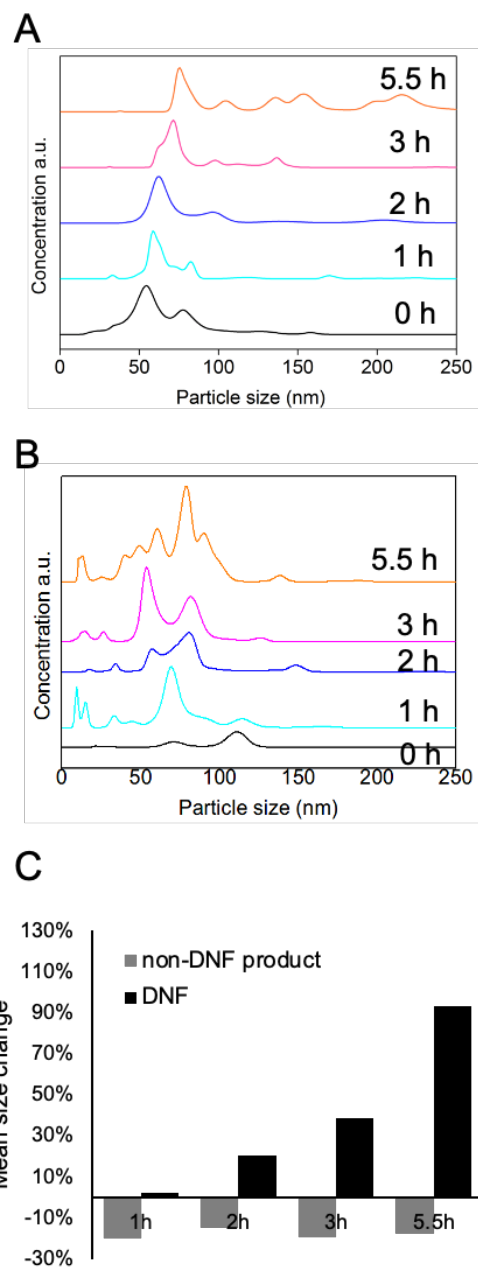


Fig. S3. Analysis of (A) DNF and (B) non-DNF with various reaction durations (0-5.5 hours). (C) Mean size change of RCA product.

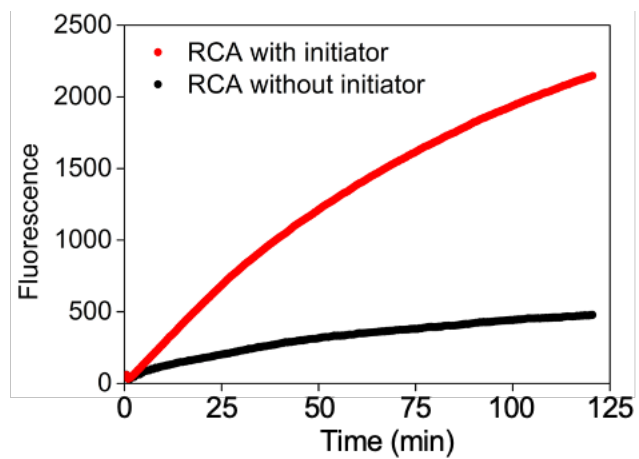


Fig. S4. Real-time fluorescence of RCA with (red) and without (black) the initiator probe added.

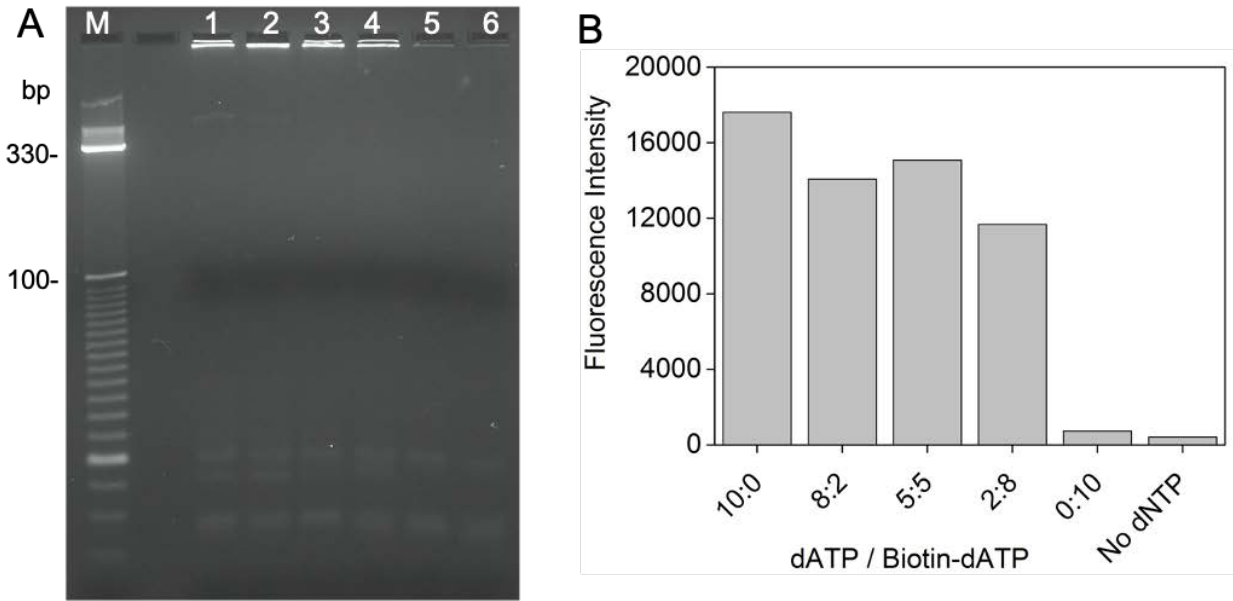


Fig. S5. RCA efficiency with different ratios of dATP to biotin-dATP added to the reaction mixture, tested by 1.5% native agarose gel (A) and represented by the fluorescence intensity detected in the wells (B).

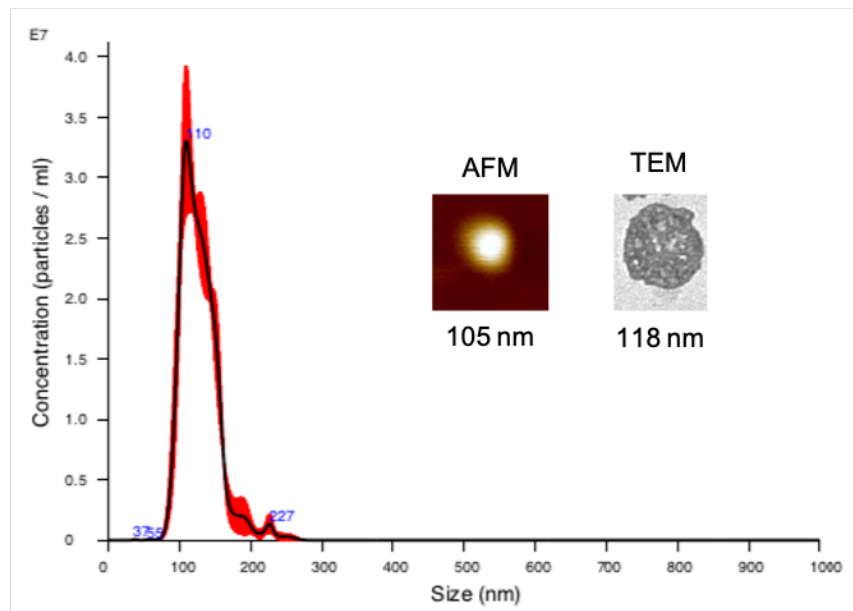


Fig. S6. NTA analysis of EV size distribution with AFM and TEM image of EV.

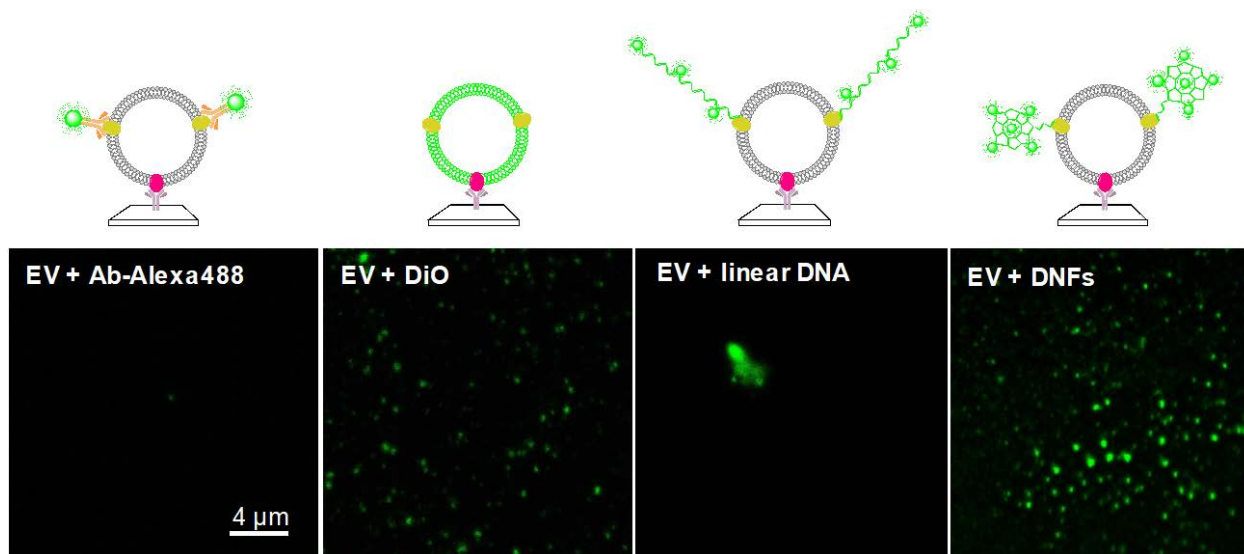


Fig. S7. Representative fluorescence microscopy images of the EVs labeled with the Alexa488 conjugated antibody, the DiO dye, the linear RCA product and the CD63-specific DNFs. All images have the same scale bar.

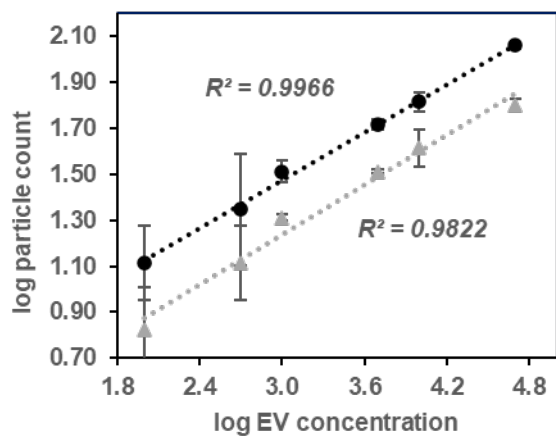


Fig. S8. Correlation between the EV particle count obtained by DiO-staining (black) or DNF-labeling (specific to HER2) (grey) and the EV input concentration, both in log scale. HER2 recognition was mediated by the anti-HER2 aptamer.

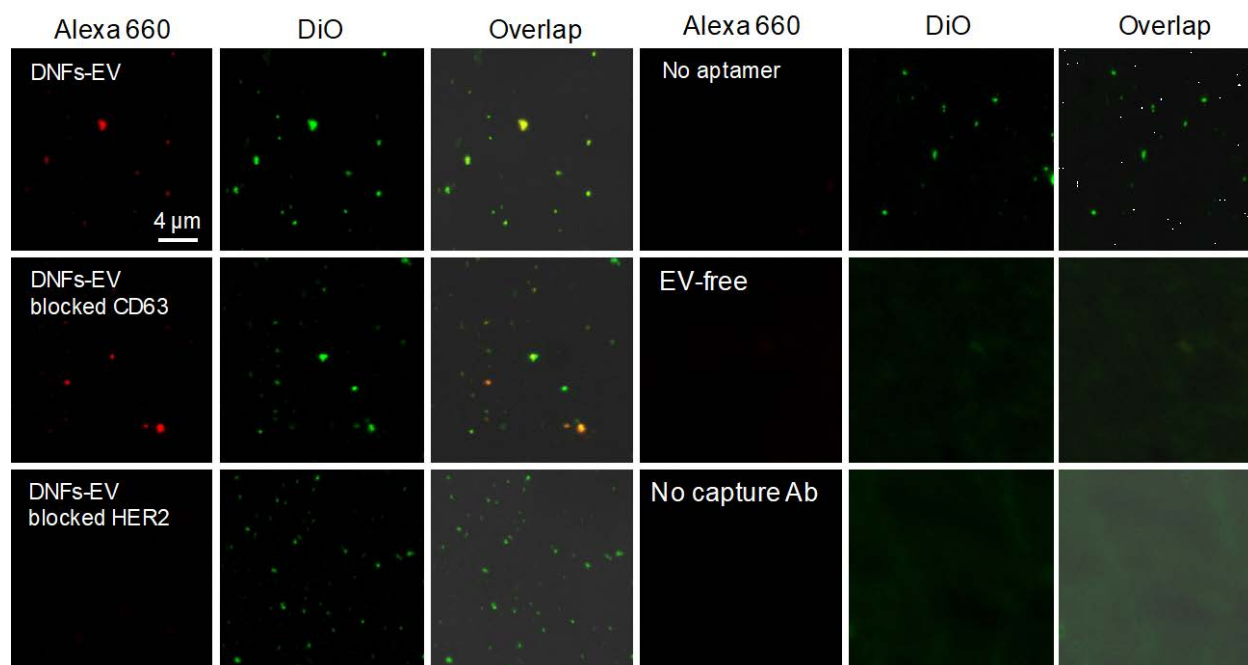


Fig. S9. Representative CFM images of different samples containing the DiO-stained EVs which were also labeled by the DNFs targeting HER2 through the anti-HER2 aptamer (DNFs-EV). Several controls were included. They were the EV samples undergoing the same DiO and DNF labeling but with the presence of 1) anti-CD63 (DNFs-EV blocked CD63) or 2) anti-HER2 (DNFs-EV blocked HER2). Or, the RCA initiator did not have the anti-HER aptamer region (No aptamer); the reaction was conducted in the EV-free sample (EV-free); or the EV sample was applied on a glass slide with no capture antibody on the surface (No capture Ab). All images have the same scale bar.

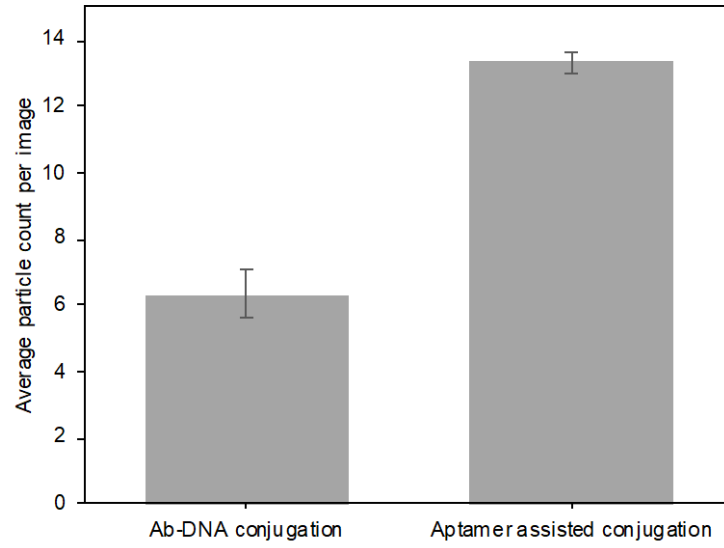


Fig. S10. Average particle count per image of found in EV samples labeled with the DNFs originated from the direct Ab-DNA conjugation and the aptamer assisted conjugation.

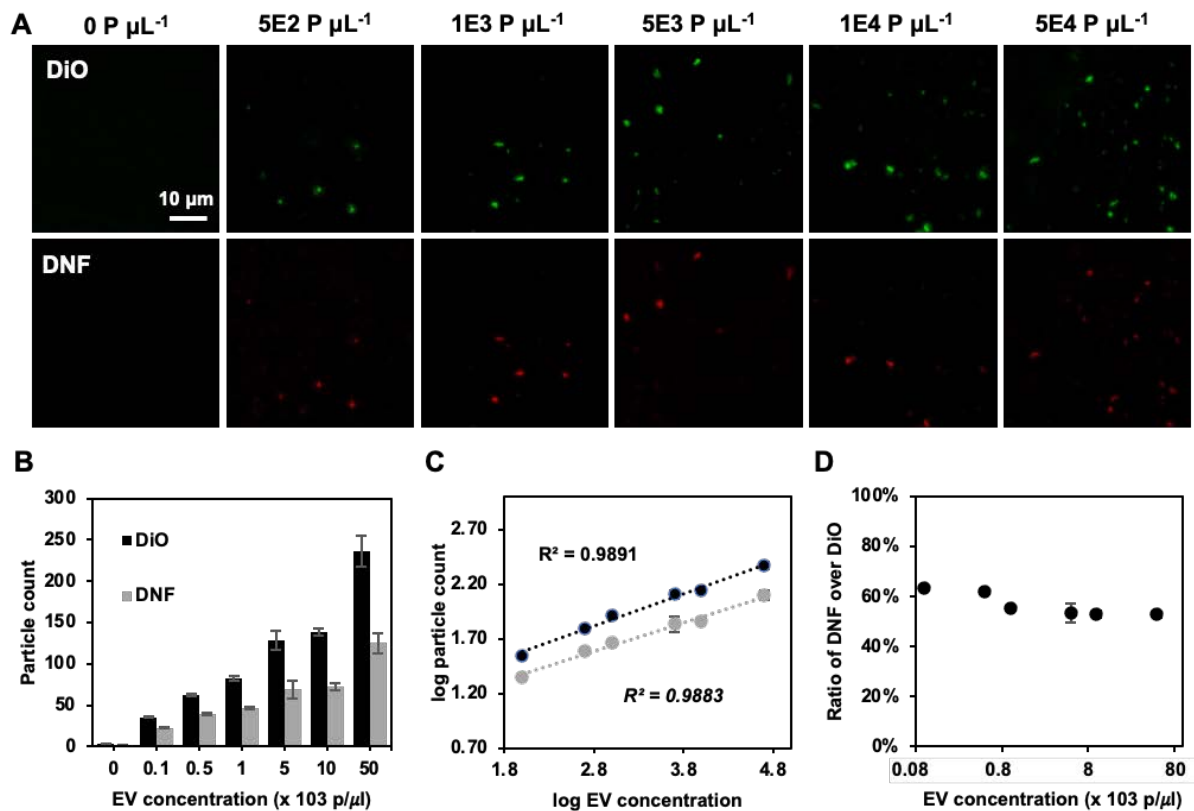


Fig. S11. Detection of EVs using dual color labeling by antibodies. (A) Representative CFM images of the EV stained by DiO and labeled by the HER2-specific DNFs with various EV input concentrations. All images share the same scale bar. (B) Particle count of the EVs labeled by DiO (black) and DNFs (grey). (C) Correlation of the EVs particle count obtained using DiO staining (black) or HER2-specific DNF labeling (grey) with the EV concentration. (D) Particle count ratio of DNFs to DiO under various EV concentrations.

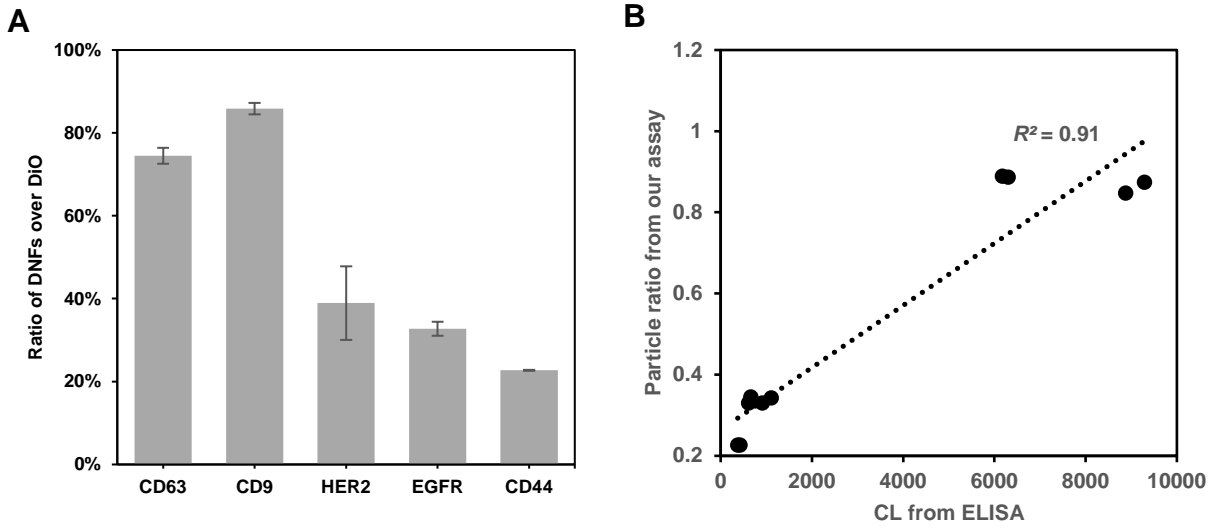


Fig. S12. (A) Comparison of the expression profiles, represented by the particle ratios, of 5 protein markers in the EVs derived from COLO-1 cells. (B) Correlation of the particle ratio obtained from our assay with the chemiluminescence signals from ELISA.

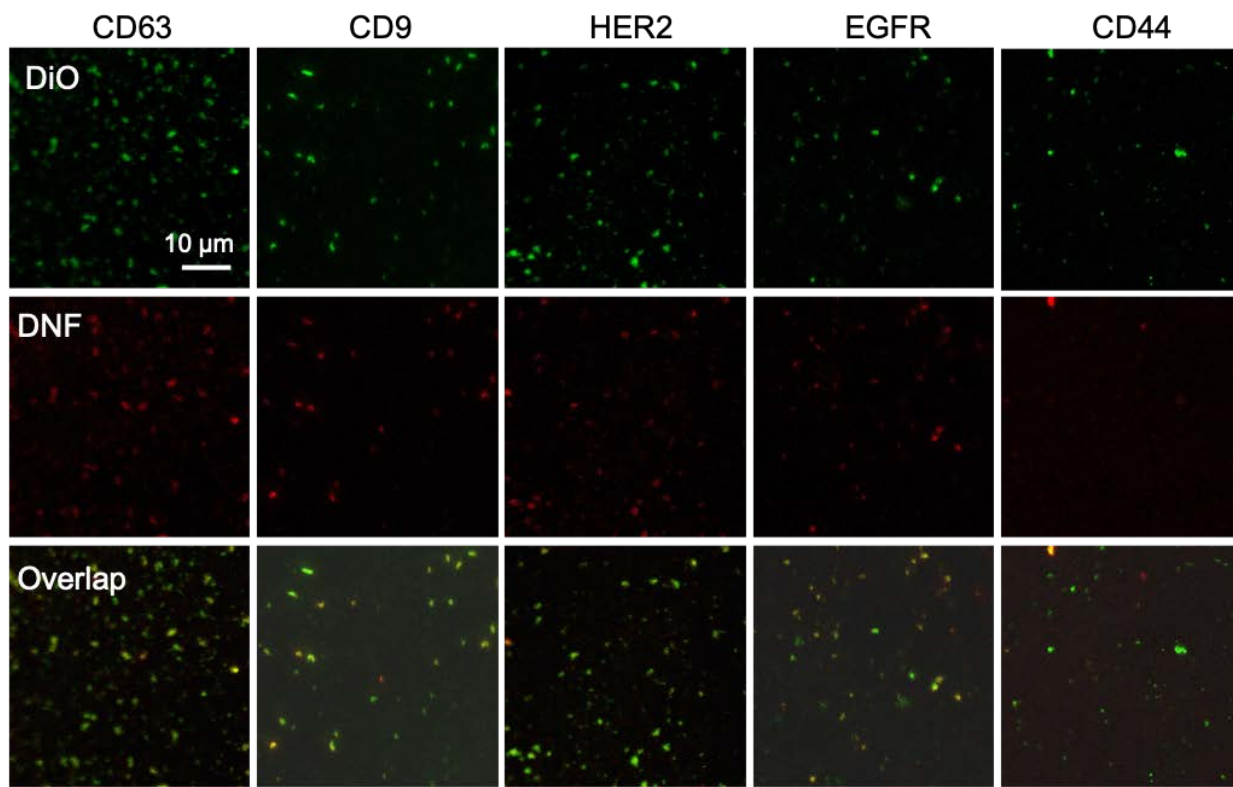


Fig. S13. Representative CFM images of the COLO-1-derived EVs labeled with the DNFs specific to CD63, CD9, HER2, EGFR and CD44. All images have the same scale bar.

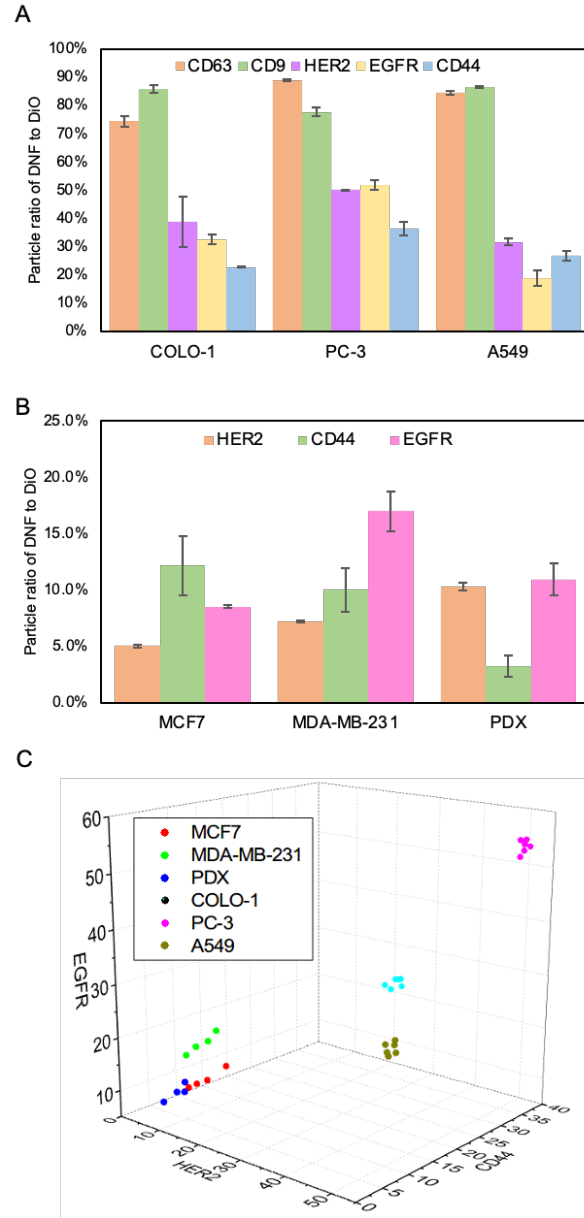


Fig. S14. (A) Comparison of the expression profiles, represented by the particle ratios, of 5 protein markers in the EVs derived from COLO-1, PC-3 and A549 cells. (B) Comparison of the expression profiles, represented by the particle ratios, of 3 protein markers in the EVs derived from MCF-7, MDA-MB-231, PDX cells. (C) The 3D plot to differentiate EVs derived from six cell lines (MCF-7, MDA-MB-231, PDX, COLO-1, PC-3, A549) using the particle counts obtained from DNF labeling targeting HER2, EGFR and CD44, respectively.

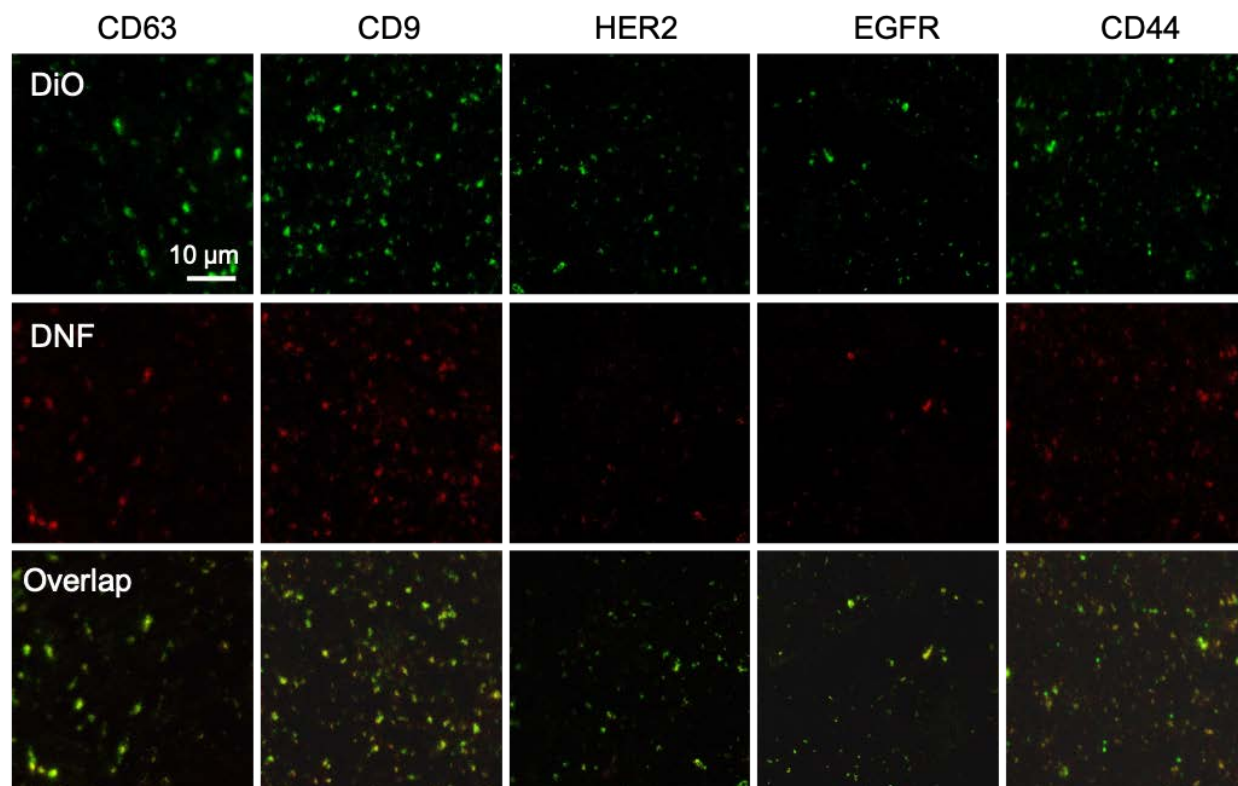


Fig. S15. Representative CFM images of the PC-3-derived EVs labeled with the DNFs specific to CD63, CD9, HER2, EGFR and CD44. All images have the same scale bar.

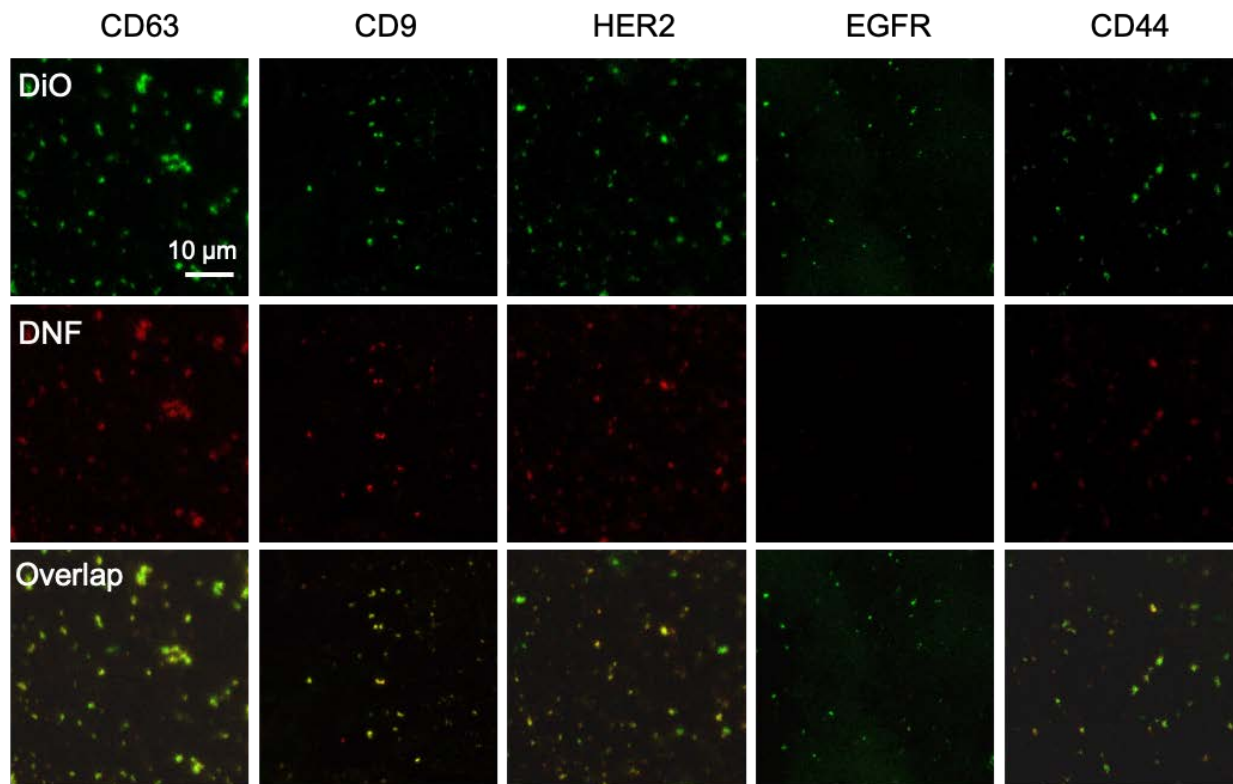


Fig. S16. Representative CFM images of the A549-derived EVs labeled with the DNFs specific to CD63, CD9, HER2, EGFR and CD44. All images have the same scale bar.

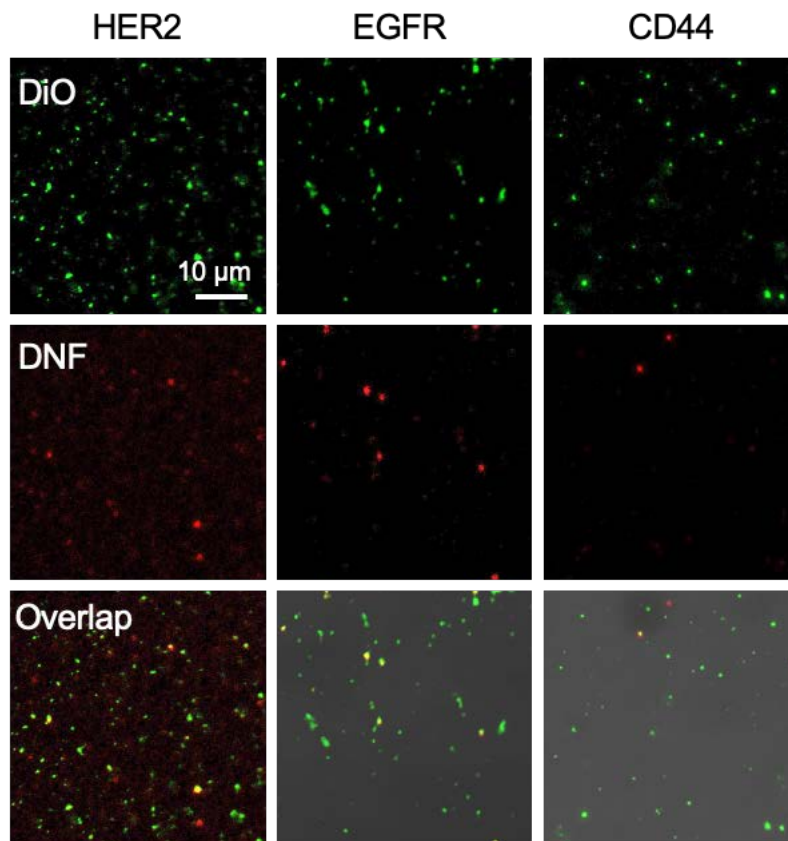


Fig. S17. Representative CFM images of the MCF-7-derived EVs labeled with the DNFs specific to CD63, CD9, HER2, EGFR and CD44. All images have the same scale bar.

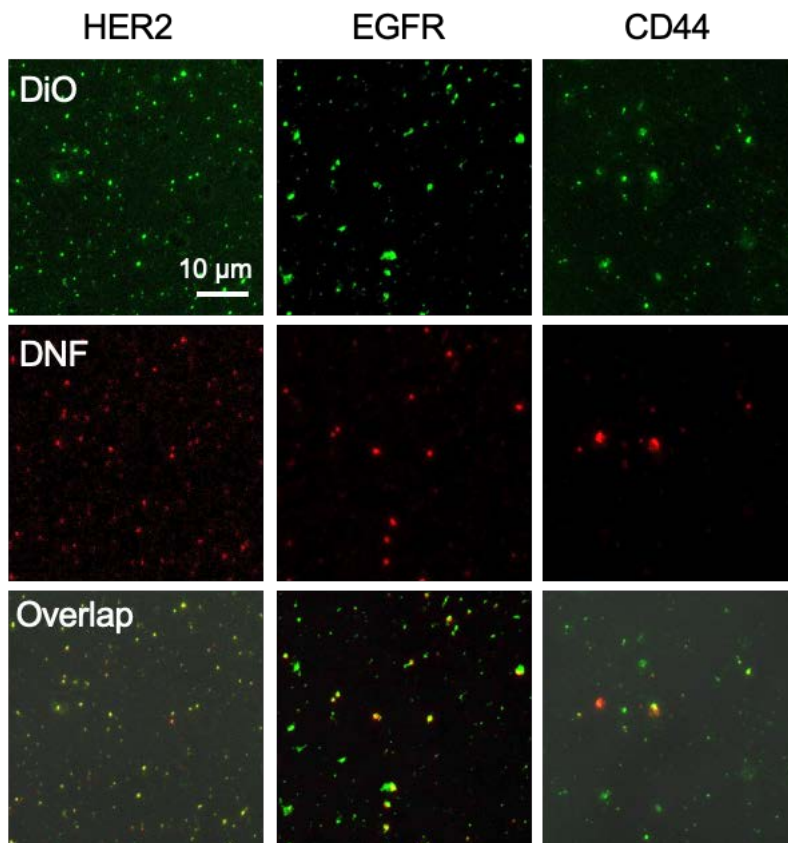


Fig. S18. Representative CFM images of the MDA-MB-231-derived EVs labeled with the DNFs specific to CD63, CD9, HER2, EGFR and CD44. All images have the same scale bar.

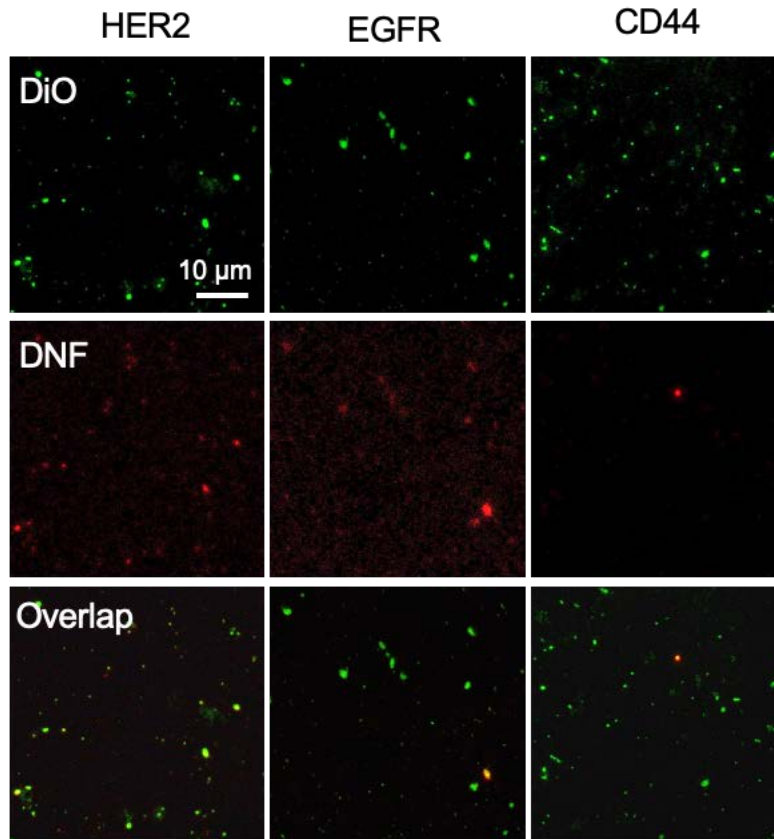


Fig. S19. Representative CFM images of the PDX-derived EVs labeled with the DNFs specific to CD63, CD9, HER2, EGFR and CD44. All images have the same scale bar.

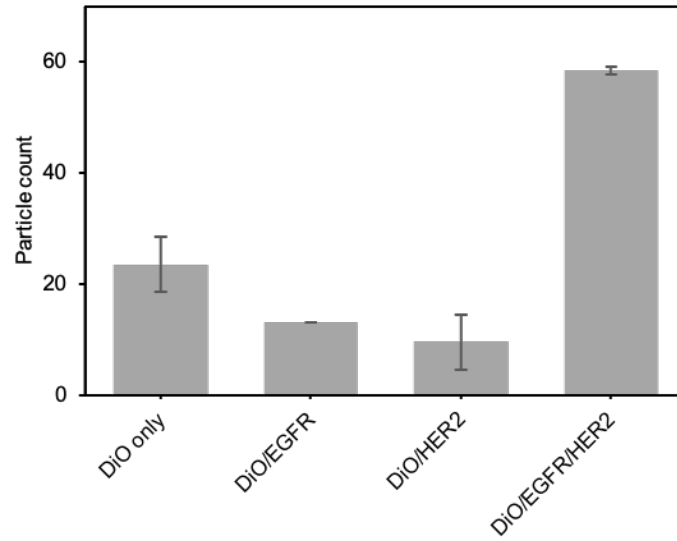


Fig. S20. Particle count of the EGFR⁻/HER2⁻ EVs, EGFR⁺/HER2⁻ EVs, EGFR⁻/HER2⁺ EVs and EGFR⁺/HER2⁺ EVs obtained with the dual marker colocalization assay.

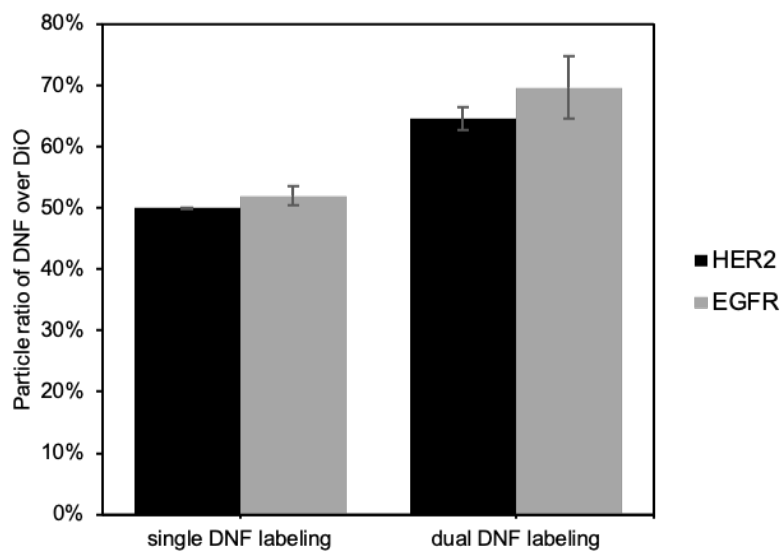


Fig. S21. Comparison of the ratio of $P_{\text{DNF}}/P_{\text{DiO}}$ obtained from single or dual DNF labeling targeting HER2 and EGFR.

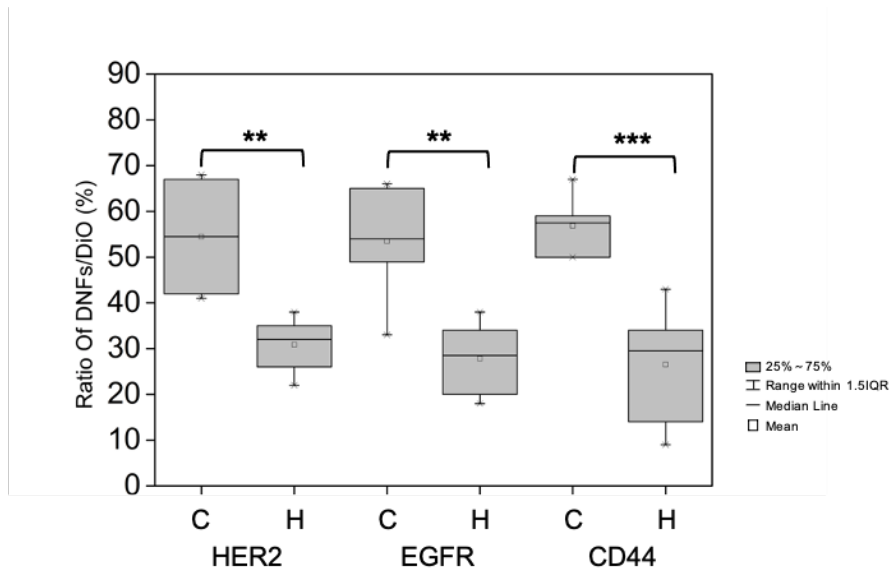


Fig. S22. Comparison of the ratio of P_{DNF}/P_{DiO} obtained by detecting the single EVs using DNFs specific to HER2, EGFR, and CD44 in the serum samples collected from breast cancer patients (C) and healthy controls (H). ** $p < 0.01$, *** $p < 0.001$.

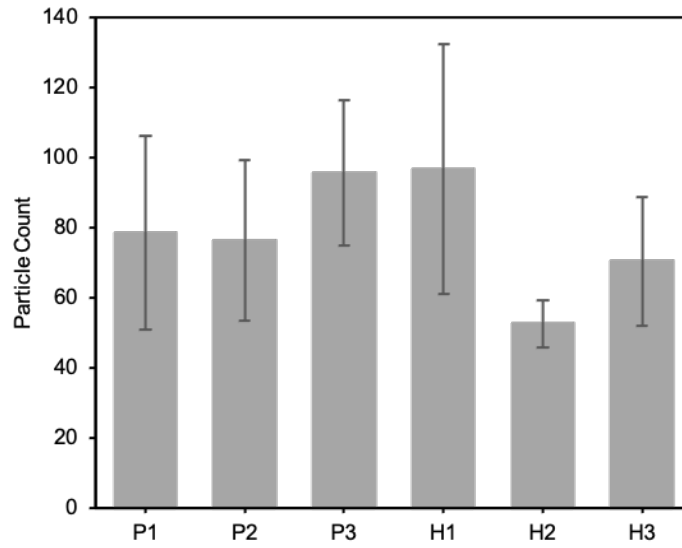


Fig. S23. Particle count of the DiO-stained EVs in the serum samples from breast cancer patients and healthy controls.

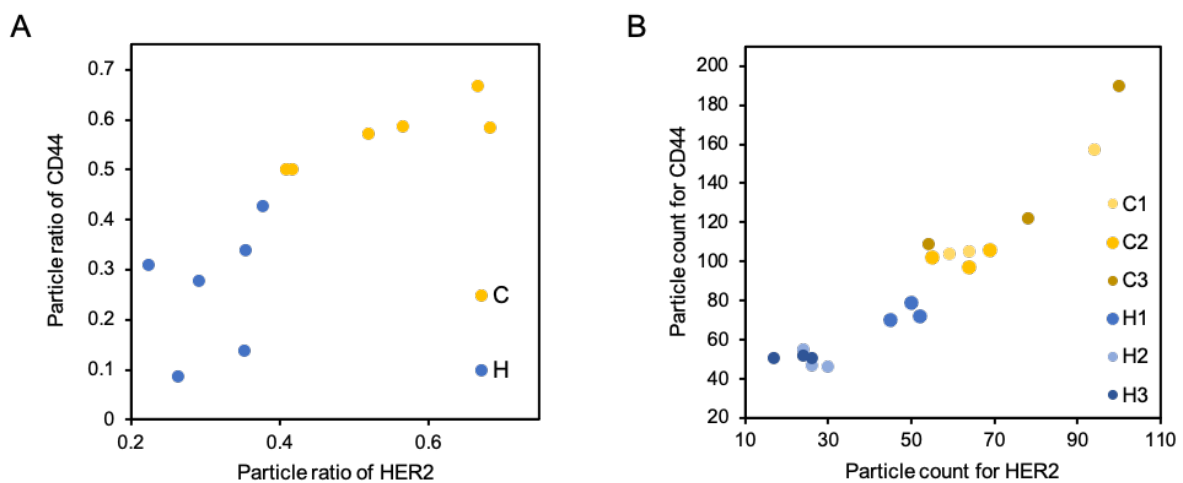


Fig. S24. EV detection by DNF labeling targeting HER2 and CD44, respectively in the serum samples from cancer patients and healthy controls. (A) Particle ratio of P_{DNF}/P_{DiO} obtained by detecting one marker at a time with the EV captured by anti-CD9 & anti-CD63. (B) Particle counts obtained by simultaneously detecting dual markers on the same EV with the EV captured by anti-CD44 and labeled by the DNF targeting HER2.